The Galactic Center as a laboratory for extreme mass ratio gravitational wave source dynamics

Tal Alexander

Weizmann Institute of Science, Faculty of Physics
The William Z. and Eda Bess Novick Career Development Chair

Abstract. The massive Galactic black hole and the stars around it are a unique laboratory for studying how relaxation processes lead to close interactions of stars and compact remnants with the central massive black hole, in particular those leading to the emission of gravitational waves. I review new results on the processes of strong mass segregation and loss-cone refilling by massive perturbers and resonant relaxation; describe observational evidence that these processes play a role in the Galactic Center and can be studied there; and discuss some of the implications for Extreme Mass Ration Inspiral event rates and their properties.

Keywords: Black hole physics – galactic center – gravitational waves – stellar dynamic
PACS: 98.62.Js, 98.35.Jk, 97.60.Lf

INTRODUCTION

The $M_\bullet \sim 4\times10^6 M_\odot$ massive black hole (MBH) in the Galactic Center (GC) [1, 2] is special not only because it is the nearest and observationally most accessible of all MBHs, but also because it is an archetype of the extragalactic MBH targets for the planned Laser Interferometer Space Antenna (LISA) gravitational wave (GW) detector. This is a coincidence: current technology limits LISA's baseline to 5×10^6 km, which happens to coincide with the typical GW wavelength emitted by an object on the last stable circular orbit around a $\sim 10^7 M_\odot$ MBH. GW from more massive MBH have longer wavelengths, beyond the sensitivity of LISA. As shown below, LISA's focus on the lower range of MBH masses implies that LISA targets will typically lie in dynamically relaxed, high density nuclei. In such systems, relaxation controls the rate at which compact remnants on wide orbits near the MBH are scattered into inspiral orbits ("loss-cone" orbits) and become extreme mass ratio inspiral (EMRI) GW sources. Thus, to understand and predict EMRI rates and orbital properties, it is necessary to understand the various dynamical relaxational processes that occur close to a MBH, and the degree of concentration of compact remnants around it. I describe here several newly (re-)discovered relaxation mechanisms beyond standard 2-body relaxation, which likely play an important role in EMRI dynamics, and discuss how these theoretical ideas are tested by observations of the GC.

NUCLEAR DYNAMICS OF LISA MBH TARGETS

LISA targets have dynamically relaxed, high density stellar cusps. This is a direct consequence of the tight empirical correlation observed between MBH masses and the

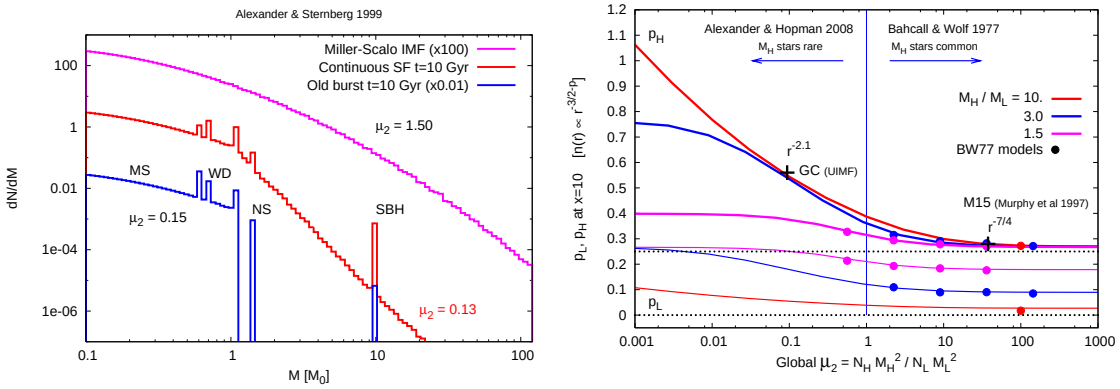

Figure 1. **Left**: Strong mass segregation. The predicted values of the global relaxational self-coupling parameter μ_2 for a "universal" Miller & Scalo IMF [8] (top line), an evolved mass function assuming continuous stars formation over 10 Gyr (middle line), and an evolved star formation burst 10 Gyr old (bottom line) [Alexander & Hopman 2008, in prep.]. The mass functions of the old populations develop excesses in the ~ 0.6–$1.4 M_\odot$ range due to the accumulation of white dwarfs and neutron stars, and in the $\sim 10 M_\odot$ range due to the accumulation of stellar black holes (here represented by a simplified discrete mass spectrum, see [9, tbl 2.1]). **Right**: Fokker-Planck mass-segregation results [Alexander & Hopman 2008, in prep.]. The logarithmic slopes p_H and p_L of the distribution functions of the heavy stars (thick lines) and light stars (narrow lines) , evaluated at ($r \sim 0.1$ pc in the GC), as function of the global relaxational self-coupling parameter μ_2, for mass ratios of M_H/M_L = 1.5, 3, 10. The cross on the left indicates the logarithmic slope of the stellar density of massive stars in the GC ($\alpha_H = 3/2 + p_H \simeq 2.2$ for $\mu_2 \sim 0.13$, see left panel), assuming a universal IMF and continuous star formation history. The cross on the right indicates the logarithmic slope for globular cluster M15, assuming it harbors an IMBH ($\alpha_H = 1.75$ estimated at $\mu_2 \sim 37$, based on a model for the cluster mass function [10]). The results for the models studies by BW76 [5] are indicated by circles.

velocity dispersion of the spheroid of their host galaxy, $M_\bullet \propto \sigma^\beta$ ($4 \lesssim \beta \lesssim 5$) [3, 4]. Here we assume for simplicity $\beta = 4$; a higher value only reinforces the following conclusions.

The MBH radius of dynamical influence is defined as $r_h \sim GM_\bullet/\sigma^2 \propto M_\bullet^{1/2}$. The mass in stars within r_h is of the order of the mass of the MBH, so their number is $N_h \sim M_\bullet/M_\star$, where $M_\star$ is the mean stellar mass, and the average stellar density there is $\bar{n}_h \sim N_h/r_h^3 \propto M_\bullet^{-1/2}$. The "$nv\Sigma$" rate of strong gravitational collisions can be used to estimate the two-body relaxation time at r_h, $T_R \sim \left[\bar{n}_h \sigma (GM_\star/\sigma^2)^2\right]^{-1} \propto M_\bullet^{5/4}$ (note for future reference that $T_R^{-1} \propto M_\star^2 N_\star$). Evaluated for the Galactic MBH, $T_R \sim O(1\,\mathrm{Gyr}) < t_H$ (the Hubble time) and $\bar{n}_h \sim O(10^5\,\mathrm{pc}^{-3})$. Note that for a MBH only a few times more massive than the Galactic MBH, $T_R \gtrsim t_H$. The GC is thus a member of a subset of galactic nuclei with relaxed, high-density stellar cusps. Such systems are expected to settle into a power-law cusp distribution, $n_\star \propto r^{-\alpha}$ [5]. Therefore, close to the MBH where EMRIs originate, $n_\star \gg \bar{n}_h$. The short relaxation time also implies that the system will not retain memory of any past major perturbations, such as a merger with a second MBH [6, 7].

STRONG MASS SEGREGATION

The degree of central concentration of compact remnants, and in particular of stellar mass BHs (SBHs), is crucial for determining the EMRI rate, since the analysis of the loss-cone refilling problem for inspiral orbits [11] shows that the rate is $\Gamma \sim N_\star(< r_{\rm crit})/T_R$, where $N_\star$ is the number of enclosed stars within $r_{\rm crit} \sim O(0.01\,{\rm pc})$, the critical radius that demarcates the boundary between SBHs that plunge (infall) directly into the MBH due to perturbations by other stars ($r > r_{\rm crit}$), and SBHs that gradually inspiral unperturbed into the MBH due to the dissipation of orbital energy by the emission of GW ($r < r_{\rm crit}$). A relaxed system is expected to undergo mass-segregation, where the massive, long-lived objects (SBHs) sink to the center, while the relatively light, long-lived objects (main-sequence dwarfs, white dwarfs and neutron stars) are pushed out.

The Bahcall-Wolf 1977 (BW77) solution [5], long-assumed to universally describe relaxed cusps around a MBH, predicts that stars in a population with masses $M_L \leq M_\star \leq M_H$ should relax to power-law cusps with a mass-dependent slope, $n_M \propto r^{-\alpha_M}$, where $\alpha_M = 3/2 + p_M$ and $p_M = M_\star/4M_H$. Thus, SBHs are predicted to have a steep $r^{-7/4}$ cusp, while the lowest-mass stars will have a flatter $r^{-3/2}$ cusp. In the single mass limit, this solution agrees with the known result $\alpha = 7/4$ [12]. However, the BW77 solution is both puzzling and problematic since (i) it does not depend at all on the mass function (apparently, even a few very massive objects can flatten the cusp of the dominant low-mass stars), and (ii) it predicts a lower degree of segregation than the strong segregation ($\alpha_{10M_\odot} > 2$) that is measured in simulations [13] and analytical models [14] of the GC. Such strong segregation is also is consistent with the observed strong central suppression of low-mass giants in the GC [15, M. Levi, MSc thesis].

A recent study of the mass segregation problem [16, Alexander & Hopman 2008, in prep.] reveals a new branch of solutions which apply in the limit where the heavy objects are relatively rare, not considered by BW76. This the generic case in old coeval or continuously star-forming populations with universal IMFs, such as observed in the GC [17]. In old populations, the initially broad mass function "polarizes" over time into two mass groups: $O(1M_\odot)$ objects (main sequence dwarfs, white dwarfs and neutron stars) and $O(10M_\odot)$ objects (SBHs) (Fig. 1 left). When the heavy objects are rare, M_H–M_L interactions dominate, leading to dynamical friction-induced sinking of the heavy stars to the center, and to the formation of a steep cusp. The relative strength of M_H–M_H scattering and M_H–M_L drag can be roughly expressed by a "relaxational self coupling parameter", $\mu_2 \equiv M_H^2 N_H / M_L^2 N_L$, where N_H/N_L is the number ratio of heavy to light stars far from the MBH, where mass segregation is negligible (cf the derivation of the relaxation time above). BW77 explored only models with $\mu_2 \gtrsim 1$, where the heavy stars dominate the dynamics and behave essentially as a single mass population. However, old populations have $\mu_2 \sim O(0.1)$ (Fig. 1 left). This leads to a much steeper mass segregation slope (Fig. 1 right), which is consistent with what is found in simulations and observations. If relaxed LISA galactic nuclei targets are similar to the GC, then the expected degree of central concentration within $r_{\rm crit}$ will be higher than previously anticipated. The implications of this for EMRI rates require further study.

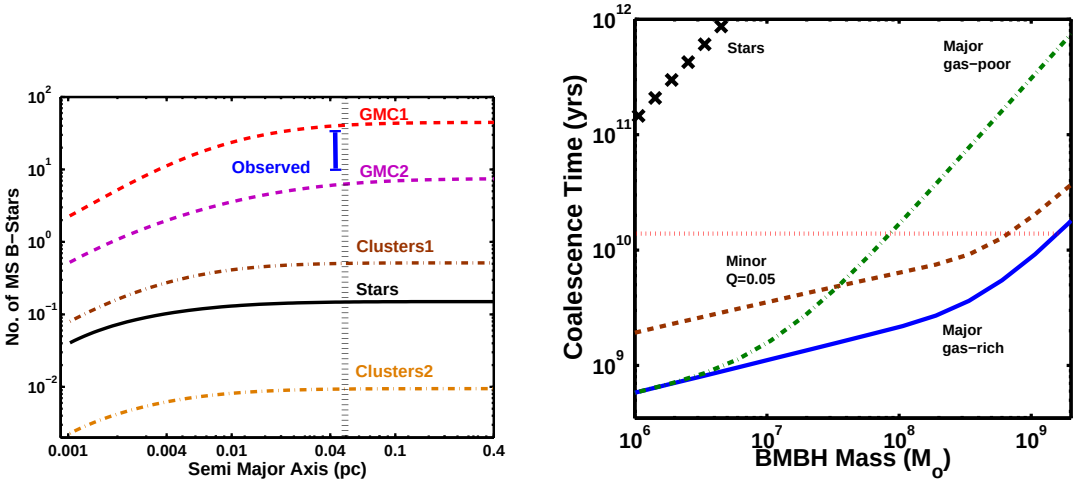

Figure 2. **Left**: A comparison between the cumulative number of S-stars (main sequence B stars) observed orbiting the Galactic MBH on randomly oriented orbits (vertical bar), and the predicted number captured by 3-body tidal interactions of the MBH with binaries detected to the center by massive perturbers, for different massive perturbers models [18]. The observed extent of the S-star cluster is indicated by the vertical hashed line. **Right**: Accelerated binary MBH mergers in the presence of MPs [19]. The time to coalescence as function of binary MBH mass, for different merger scenarios distinguished by the mass ratio Q between the two MBHs and the MP contents of host galaxies. The age of the universe is indicated by the dotted horizontal line. Stellar relaxation alone cannot supply a high enough rate of stars for the slingshot mechanism to complete the merger within a Hubble time. However, in minor mergers ($Q = 0.05$) and major gas-rich mergers ($Q = 1$) with MPs, merger is possible within a Hubble time for all but the most massive MBHs. (Reproduced with permission from the *Astrophysical Journal*)

MASSIVE PERTURBERS

The $T_R^{-1} \propto M^2 N$ scaling of the relaxation rate implies that a few very massive perturbers (MPs) of mass $M_p \gg M_\star$, such as clusters, giant molecular clouds (GMCs), or intermediate mass BHs (if those exist), may well dominate the relaxation and fundamentally affect the loss-cone refilling rate, if $\mu_2 = M_P^2 N_P / M_\star^2 N_\star \gg 1$. For example, there are $O(100)$ GMCs with masses $10^4 \lesssim M_p \lesssim 10^7\, M_\odot$ observed in the central ~ 100 pc of the Galaxy [20], as compared to $N_\star \sim 10^8$ solar mass stars, so $100 \lesssim \mu_2 \lesssim 10^8$ on that scale.

We show [18] that MPs, which affect the dynamics on the $r_{\rm MP} \gtrsim$ few pc scale (GMCs are tidally disrupted closer in), strongly increase the rate of close interactions with loss-cone processes for which $r_{\rm crit} > r_{\rm MP}$. MPs are thus not relevant for EMRIs, which are scattered singly into inspiral orbits from $r_{\rm crit} \sim O(0.01\,{\rm pc})$, or for tidally disrupted stars, which originate from $\sim r_h < r_{\rm MP}$ [21]. However, the rates of close interactions that occur at larger periapse and so have a larger $r_{\rm crit}$, such as the tidal separation of binary by the MBH, are strongly enhanced by MPs. The tidal separation of a binary with mass M_2 and semi-major axis a_2 by an MBH of mass $M_\bullet$ results in the capture of one star on a tight and eccentric orbit with semi-major axis $\langle a \rangle \sim 0.6 (M_\bullet / M_2)^{2/3} a_2$, and eccentricity $\langle e \rangle \sim 1 - 2 (M_2 / M_\bullet)^{1/3}$, and the ejection of the other star at an extremely high velocity, $v_\infty^2 \sim \sqrt{2} G M_2^{2/3} M_\bullet^{1/3} / a_2$, which exceeds the escape velocity from the Galaxy [22]. MP-

induced scattering of massive binaries from the field toward the Galactic MBH and their ensuing tidal separation can naturally explain [18] the number and spatial extent of the mysterious cluster of young stars observed within few $\times$ 0.01 pc of the Galactic MBH [1] (Fig. 2, left), as well as the number of hyper-velocity stars observed at distances of tens of kpc from the GC, on their way out of the Galaxy [23].

If typical LISA targets are similar to the Galaxy, then binaries containing compact object, which are scattered to the MBH by MPs and tidally separated, will increase the EMRI rate from WDs by an order of magnitude relative to that of singly scattered EMRIs [Perets, Hopman & Alexander, 2008, in prep.].

The orbital decay of a binary MBH in a post-merger galaxy by 3-body interactions with stars scattered into its orbit ("the slingshot effect") is another large loss-cone process that is accelerated by MPs. Binary MBH coalescence events are predicted to be the strongest sources of GW in the universe, observable by LISA from extremely high redshifts, tracing the galactic merger history and growth history of MBHs. Dynamical simulations indicate that binary MBHs in spherically symmetric systems with no gas on small scales ("dry mergers") stall, and do not reach within a Hubble time the final rapid phase of GW dissipation leading to coalescence [24]. This situation, known as the "last pc problem" is circumvented by MPs on large scales, which can efficiently scatter stars into the binary's orbit, in all but the most massive galaxies [19] (Fig. 2, right).

RESONANT RELAXATION

Two-body relaxation, or non-coherent relaxation (NR), is inherent to any discrete large-N system, due to the cumulative effect of uncorrelated two-body encounters. These cause the orbital energy E and the angular momentum J to change in a random-walk fashion ($\propto \sqrt{t}$) on the typically long NR timescale $T_{\rm NR}(r) \simeq (M_\bullet/M_\star)^2 P/N_\star \log N_\star$, where P is the orbital time at radius r and $N_\star$ the number of stars enclosed there. In contrast, when the gravitational potential has approximate symmetries that restrict orbital evolution (e.g. fixed ellipses in a Keplerian potential; fixed orbital planes in a spherical potential), the perturbations on a test star are no longer random, but correlated, leading to coherent ($\propto t$) torquing of J on short timescales, while the symmetries hold. Over longer times, this results in resonant relaxation (RR) [25, 27], a rapid random walk of J on the typically short RR timescale $T_{\rm RR} \ll T_{\rm NR}$.

The properties and timescales of RR depend on the symmetries of the potential and the processes that break them. RR in a near-Keplerian potential can change both the direction and magnitude of $\mathbf{J}$ ("scalar RR"), thereby driving stars to near-radial orbits that interact strongly with the MBH. Far from the MBH, coherent torquing is limited by orbital precession due to the enclosed stellar mass, and the resulting scalar RR timescale is $T^J_{\rm RR} \simeq (M_\bullet/M_\star)P$. Close to the MBH, where General Relativistic (GR) precession limits the coherent torquing, $T^J_{\rm RR} \simeq (3/8)(M_\bullet/M_\star)^2 (J_{\rm LSO}/J)^2 P/N_\star$, where $J_{\rm LSO} = 4GM_\bullet/c$ is the angular momentum of the last stable orbit. The combined effects of mass and GR precession result in a minimal RR timescale, $\min T^J_{\rm RR} \ll T_{\rm NR}$, at $r \sim O(0.01)$ pc for a typical LISA target, which happens to coincide with $r_{\rm crit}$ for inspiral [26] (Fig. 3, right). Thus, it is scalar RR, and not NR, that dominates EMRI dynamics. RR in a near-spherical potential (as is most likely the case anywhere within

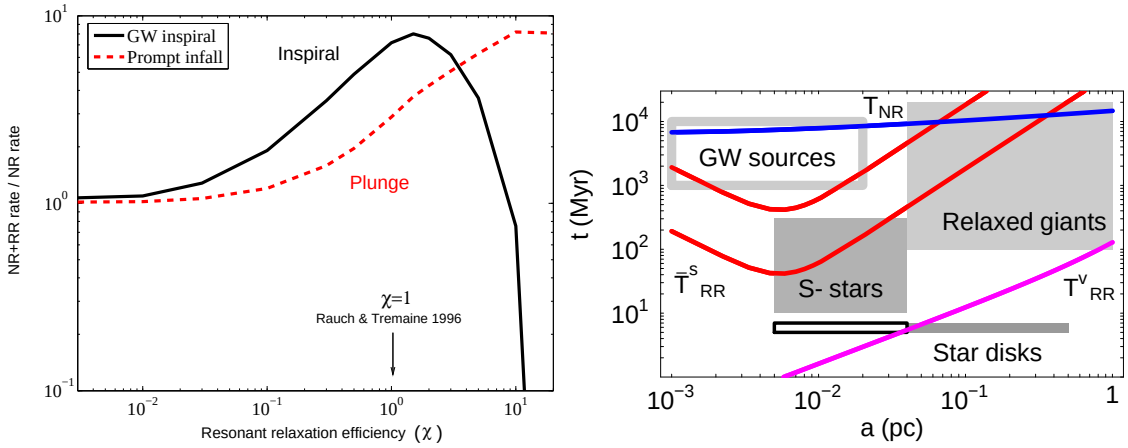

Figure 3. **Left**: Resonant relaxation efficiency. The relative rates of GW EMRI events and direct infall (plunge) events, as function of the unknown efficiency of RR, χ, normalized to $\chi = 1$ for the values derived by Rauch & Tremaine [25]. **Right**: Evidence for resonant relaxation in the GC in the plane of age .vs. distance from the MBH. The spatial extent and estimated age of the various dynamical sub-populations in the GC (shaded areas) is compared with the NR timescale (top line, for assumed mean mass of $M = 1\,M_\odot$) and with the scalar RR timescale (two curved lines, top one for $\chi M_\star = 1\,M_\odot$, bottom one for $\chi M_\star = 10 M_\odot$) and vector RR timescale (bottom line, for $\chi M_\star = 1\,M_\odot$). The populations include the young stellar rings in the GC (filled rectangle in the bottom right); the S-stars, if they were born with the disks (open rectangle in the bottom left); the maximal lifespan of the S-stars (filled rectangle in the middle left); the dynamically relaxed red giants (filled rectangle in the top right); and the reservoir of GW inspiral sources, where the age is roughly estimated by the progenitor's age or the time to sink to the center (open rectangle in the top left). Stellar components that are older than the various relaxation times must be randomized [26]. (Reproduced with permission from the *Astrophysical Journal*)

r_h) can only change the direction of **J** ("vector RR"). Coherent torquing is limited by vector RR itself, which randomizes the orbital planes (alternatively, this can be viewed as the result of potential fluctuations due to the finite number of stars), and results in $T^{\mathbf{J}}_{\rm RR} \simeq 2(M_\bullet/M_\star)P/\sqrt{N_\star}$.

There are as yet only a few quantitative studies of RR. While the effect is clearly seen in N-body simulations [25, 28], systematic studies of RR efficiency and its dependence on the properties of the stellar cusp around the MBH, and on the orbital parameter of the torqued star, are only now yielding first results [29, 28]. Determining the exact value of RR efficiency (parametrized by a dimensionless order unity coefficient χ, Fig. 3) is crucial for predicting its effects on EMRI rates. RR can increase the EMRI rate by rapidly deflecting stars to near-radial inspiral orbits that lead to quasi-periodic GW signals. However, if RR is too efficient, then it strongly suppresses the EMRI rate from single compact objects by throwing all compact objects within $r_{\rm crit}$ directly into the MBH, producing instead short, hard to detect GW bursts [26] (Fig. 3, left). The effect of strong RR on EMRIs from tidally separated binaries (see above) has yet to be investigated in detail. Recent numerical studies indicate an RR efficiency of $\chi \simeq 4$, which corresponds to an RR enhancement of the EMRI rate by a factor of few over that predicted for NR only [28].

The fact that scalar RR is quenched by GR precession when $J \rightarrow J_{\rm LSO}$, a limit that also

coincides with the stage where GW dissipation becomes important, is another crucial but still little-studied aspect of EMRI dynamics. This is important because GR quenching allows compact remnants to be deflected very rapidly by RR to strongly relativistic orbits, but then stall ''on the brink'' and instead of falling directly into the MBH, inspiral into it gradually as EMRIs.

The systematic dynamical differences between the various stellar components observed in the GC (the young central S-star cluster in the inner few $\times 0.01$ pc, the disk(s) of very massive young stars on the ~ 0.05–0.5 pc scale, and the $\lesssim$ few $\times 10^9$ yr old population of isotropic red giants) can be explained by the effects of RR (Fig. 3, right). In particular, the truncation of the star disk(s) at ~ 0.04 pc is consistent with scalar RR with $\chi \sim O(1)$, and the relaxed population of red giants is consistent with the effects of vector RR. Thus, observations of the GC can provide an empirical test of the RR concept and constrain its efficiency.

SUMMARY

The empirical $M_\bullet/\sigma$ relation implies that LISA extragalactic targets, MBHs in the range $M_\bullet \lesssim 10^7\,M_\odot$, lie in very high density relaxed stellar cusps. The Galactic MBH happens to be an archetype of LISA targets. In such systems, it is the slowest relaxation process, non-coherent 2-body relaxation, or possibly other more efficient processes, that determine the central concentration of compact EMRI candidates, and the rate at which they are captured in EMRI orbits. We described several new results on processes that may strongly affect the cosmological EMRI rates, and can be tested by observations of the GC: strong mass segregation, which drives heavy SBHs into unusually high concentrations near the MBH, and may have left an imprint in the strong observed central suppression of light giants around the Galactic MBH; accelerated loss-cone refilling by massive perturbers, which strongly affects the rate at which binaries are tidally separated by the MBH, leaving compact objects very close to the MBH. This mechanism very naturally explains the cluster of young stars around the Galactic MBH and the numbers of hyper-velocity stars observed on their way out of the Galaxy; and RR, which dominates EMRI dynamics and likely enhances their rate. RR can explain some of the systematic differences between the dynamical properties of the various stellar populations observed in the GC, and conversely, these observations can be used to test this process and constrain its properties.

The implications of all these processes on the EMRI rates have still to be fully mapped. However, it is already safe to say that GW astronomy will tell us as much about fundamental questions in stellar dynamics, as it will tell us about cosmology and GR.

ACKNOWLEDGMENTS

This work was supported by ISF grant 928/06, Minerva grant 8563 and a New Faculty grant by Sir H. Djangoly, CBE, of London, UK.

REFERENCES

1. F. Eisenhauer, et al., *ApJ* **628**, 246–259 (2005).
2. A. M. Ghez, S. Salim, S. D. Hornstein, A. Tanner, J. R. Lu, M. Morris, E. E. Becklin, and G. Duchêne, *ApJ* **620**, 744–757 (2005).
3. L. Ferrarese, and D. Merritt, *ApJ* **539**, L9–L12 (2000).
4. K. Gebhardt, et al., *ApJ* **539**, L13–L16 (2000).
5. J. N. Bahcall, and R. A. Wolf, *ApJ* **216**, 883–907 (1977).
6. D. Merritt, and A. Szell, *ApJ* **648**, 890–899 (2006).
7. D. Merritt, S. Mikkola, and A. Szell, *ApJ* **671**, 53–72 (2007).
8. G. E. Miller, and J. M. Scalo, *ApJS* **41**, 513–547 (1979).
9. T. Alexander, *Physics Reports* **419**, 65–142 (2005).
10. B. W. Murphy, H. N. Cohn, P. M. Lugger, and G. A. Drukier, "The Stellar Mass Function of the Globular Cluster M15," in *Bulletin of the American Astronomical Society* **29**, 338–+ (1997).
11. C. Hopman, and T. Alexander, *ApJ* **629**, 362–372 (2005).
12. J. N. Bahcall, and R. A. Wolf, *ApJ* **209**, 214–232 (1976).
13. M. Freitag, P. Amaro-Seoane, and V. Kalogera, *ApJ* **649**, 91–117 (2006).
14. C. Hopman, and T. Alexander, *ApJ* **645**, L133–L136 (2006).
15. R. Schödel, et al., *A&A* **469**, 125–146 (2007).
16. T. Alexander, "Stellar Relaxation Processes Near the Galactic Massive Black Hole," in *2007 STScI Spring Symposium: Black Holes*, edited by M. Livio, and A. Koekemoer, Cambridge University Press, 2007, in press, `arXiv:astro-ph/0708.0688`.
17. T. Alexander, and A. Sternberg, *ApJ* **520**, 137–148 (1999).
18. H. B. Perets, C. Hopman, and T. Alexander, *ApJ* **656**, 709–720 (2007).
19. H. B. Perets, and T. Alexander, *ApJ* **677**, 146–159 (2008).
20. T. Oka, T. Hasegawa, F. Sato, M. Tsuboi, A. Miyazaki, and M. Sugimoto, *ApJ* **562**, 348–362 (2001).
21. A. P. Lightman, and S. L. Shapiro, *ApJ* **211**, 244–262 (1977).
22. J. G. Hills, *Nature* **331**, 687–689 (1988).
23. W. R. Brown, M. J. Geller, S. J. Kenyon, and M. J. Kurtz, *ApJ* **622**, L33–L36 (2005).
24. D. Merritt, and M. Milosavljević, *Living Reviews in Relativity* **8**, 8–+ (2005).
25. K. P. Rauch, and S. Tremaine, *New Astronomy* **1**, 149–170 (1996).
26. C. Hopman, and T. Alexander, *ApJ* **645**, 1152–1163 (2006).
27. K. P. Rauch, and B. Ingalls, *MNRAS* **299**, 1231–1241 (1998).
28. E. Eilon, G. Kupi, and T. Alexander, The efficiency of resonant relaxation around a massive black hole (2008), submitted to ApJ , `arXiv:astro-ph/0807.1430`.
29. M. A. Gürkan, and C. Hopman, *MNRAS* **379**, 1083–1088 (2007).